Cosmological Consequences of Massive Gravity

Tina Kahniashvili
Carnegie Mellon University
Ilia State University

Tbilisi
September 27, 2017

Outline

- Motivations to consider beyond the standard cosmological model
  - Cosmological constant problem
  - CMB large scale anomalies
- Massive cosmologies
  - dRGT
  - Extended quasi-dilaton models
- Cosmological signatures
  - CMB temperature and polarization anisotropies
  - Large scale structure

Collaboration

- Nishant Agarwal (UM-Lowell)
- Arjun Kar (U-Penn)
- Arthur Kosowsky (University of Pittsburgh)
- George Lavrelashvili (RMI, TSU & Max-Planck)
- Paul Rogozenski (Carnegie-Mellon University)
- Dacen Waters (Carnegie-Mellon University)

Kahniashvili, Kar, Lavrelashvili, Agarwal et al. 2015

Precise Cosmology

- **Observations – 1% precision**
- **Theory – unknown 96% (Dark Universe)**

The cosmological constant problem

10^{120} times lighter than we can expect from the theory M_{pl}^4

"Einstein's Greatest Blunder"

"The worst theoretical prediction in the history of physics!"
Hobson, Efstathiou & Lasenby

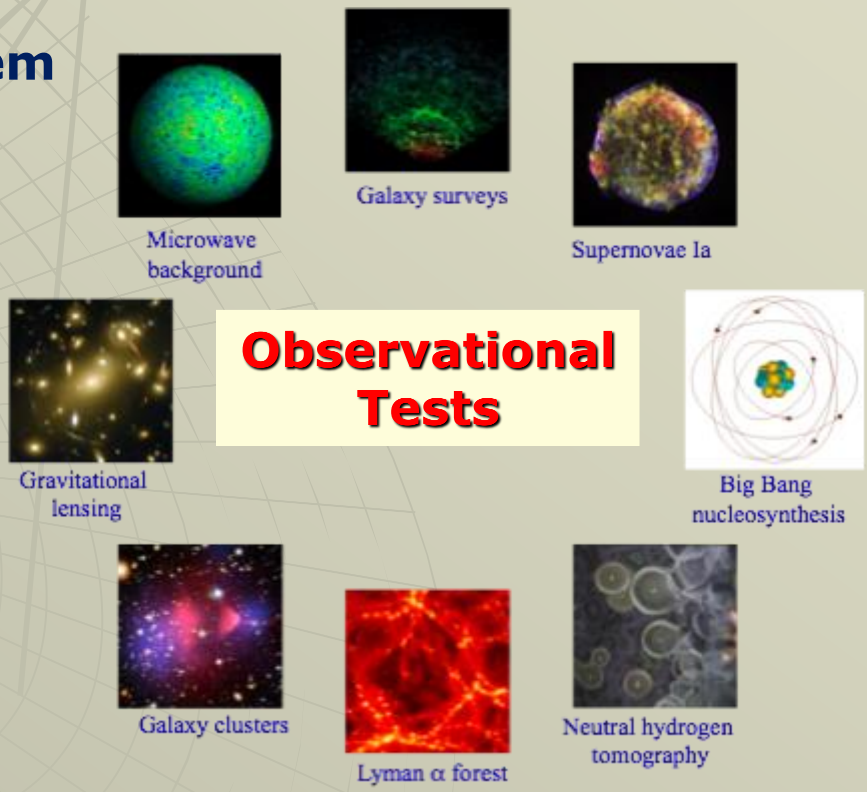

Do We Need New Physics

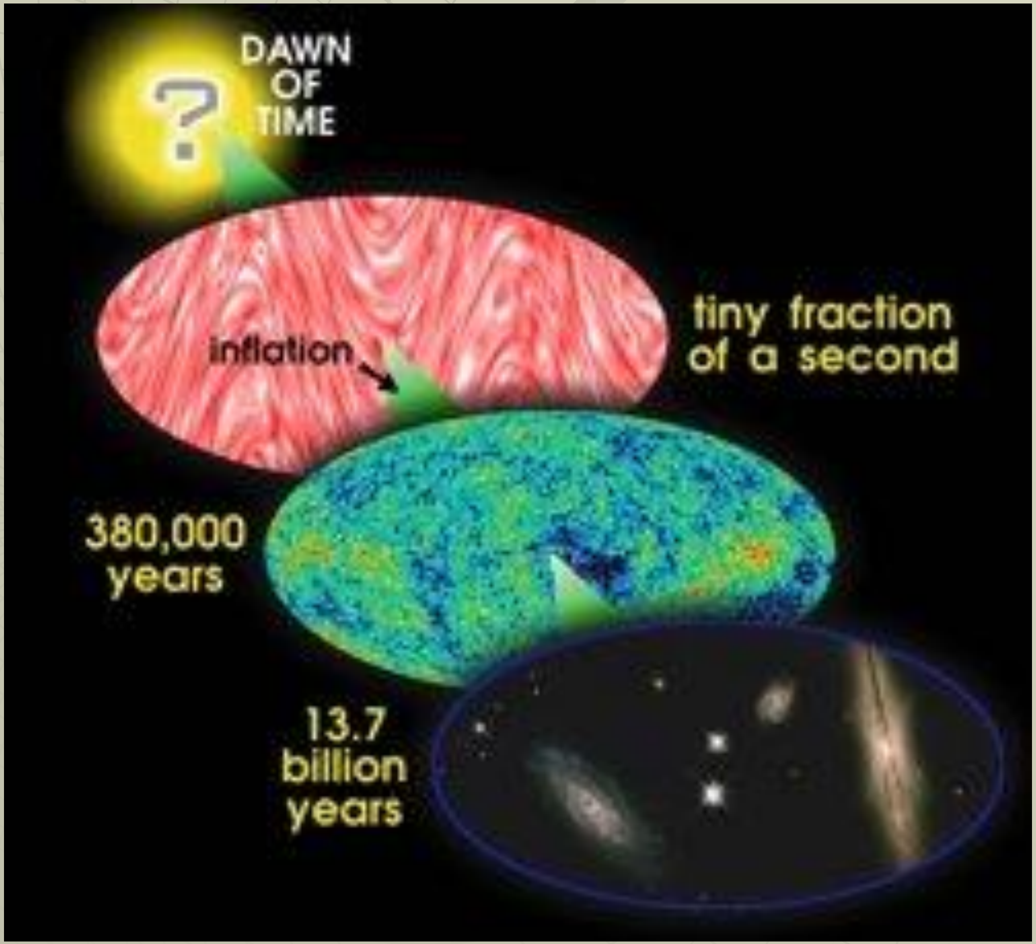

CMB Anomalies

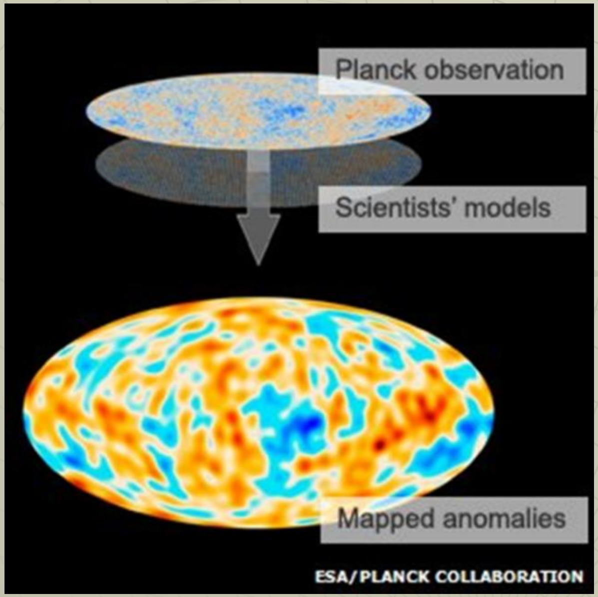

- Anomalies at Large Scales
  - North-South Asymmetries
  - Power Suppression
  - Multipole Alignments
  - Cold Spot

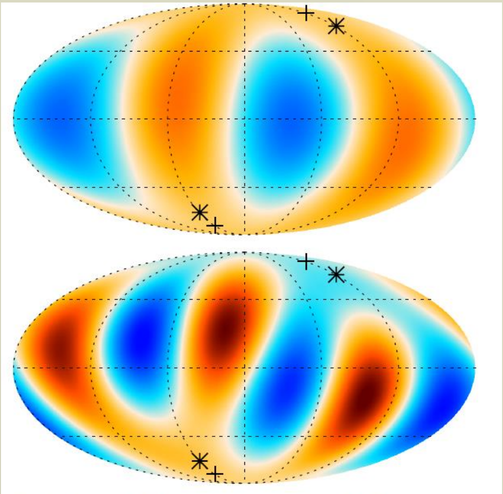

Fig. 20. Upper: The Wiener filtered SMICA CMB sky (temperature range ± 400 μK). Middle: the derived quadrupole (temperature range ± 35 μK). Lower: the derived octopole (temperature range ± 35 μK). Cross and star signs indicate axes of the quadrupole and octopole, respectively, around which the angular momentum dispersion is maximized.

Cope,. Huterer, Schwarz & Starkman, 2008

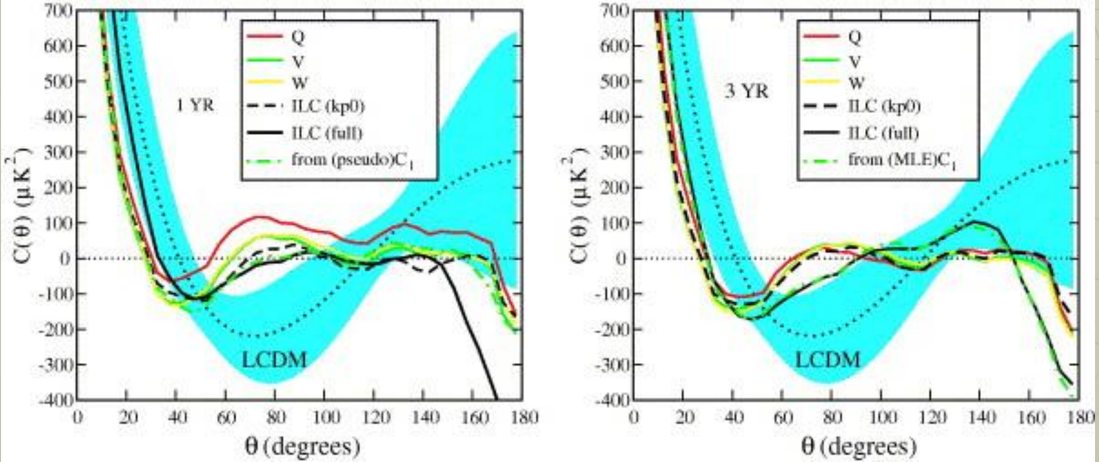

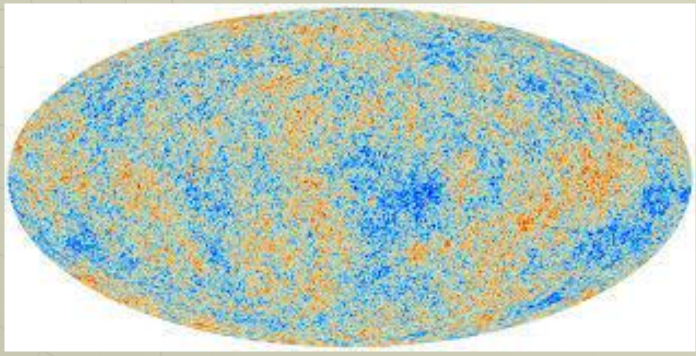

Massive Gravity

- **Motivation**

Alternative explanation of accelerated expansion of the Universe: Massive graviton spin0 mode mimics the presence of Dark Energy

✧deRham, Gabadadze, Tolley 2010 $m \sim H_0$

- **Theoretical Foundation**

✧DeRham, Gabadadze, Tolley 2010

$$\rho_{co} \equiv 3M_{Pl}^2 m^2.$$

- **Massive Cosmologies**

Two stages: at high densities (above cross-over) – isotropic model, at low densities (below cross-over)– non-existence of isotropic solutions

✧D'Amico, deRham, Dubovsky, Gabadadze, Pirtskhalava, Tolley 2011

Massive Gravity: History

- ***Fierz & Pauli, 1939***
  - Non-zero graviton mass
- ***van Dam & Veltman, 1970; Zakharov, 1970***
  - vDVZ discontinuity (GR is not recovered in

    m->0 limit)
- ***Vainstein 1972***
  - vDVZ discontinuity disappears if we take into account non-linear interactions of the scalar mode
- ***Boulware & Deser, 1972***
  - Sixth degree of freedom - ghost

Massive Cosmologies

- **dRGT** – 4D covariant, nonlinear, ghost free at decoupling limit at all orders
  - **m~H_0**
- **Quasi-Dilaton**
  - *D'Amico, Gabadadze, Hui, Pirtskhalava, 2012 (1206.4253)*
  - *De Felice et al. 2013 (1305.5502)*
- **Vainstein radius**

$$r_* = \left(\frac{r_g}{m^2}\right)^{1/3} = \left(\frac{\rho}{3M_{\rm Pl}^2 m^2}\right)^{1/3} R,$$

- **Mass varying theory**
  - *Huang, Piao, Zhou, 2012 (1206.5678)*

Extended Quasidilaton Massive Gravity

De Felice and Mukohyama 2013

$$H \equiv \frac{\dot{a}}{Na}\,,$$

$$X \equiv \frac{e^{\bar{\sigma}/M_{\rm Pl}}}{a}\,,$$

$$r \equiv \frac{n}{N}\,a\,.$$

$$S = \frac{M_{\rm Pl}^2}{2}\int d^4x\sqrt{-g}\Big[R - 2\Lambda - \frac{\omega}{\ldots}\partial_\mu\sigma\partial^\mu\sigma$$

$$+2m_g^2(\mathcal{L}\ldots$$

$$\left(\frac{\dot{\phi}^0}{n}\right)^2 \equiv 1 - \alpha_\sigma\left(\frac{\dot{\sigma}}{qXm_g}\right)^2\,,$$

$$J \equiv 3 + 3(1-X)\alpha_3 + (1-X)^2\alpha_4\,.$$

$$\Lambda_X \equiv m_g^2(X-1)[6-3X + (X-4)(X-1)\alpha_3 + (X-1)^2\alpha_4]\,.$$

$$r = 1 + \frac{\omega H^2}{m_g^2 X^2[\alpha_3(X-1)-2]}\,,$$

$$\left(3 - \frac{\omega}{2}\right)H^2 = \Lambda + \Lambda_X\,,$$

$$\left(\frac{\dot{\phi}^0}{n}\right)^2 \equiv 1 - \alpha_\sigma\left(\frac{\dot{\sigma}}{qXm_g}\right)^2\,,$$

Tensor Massive Mode

De Felice and Mukohyama 2013

$$M_{\rm GW}^2 \equiv \frac{(r-1)X^3 m_g^2}{X-1} + \frac{\omega H^2 (rX + r - 2)}{(X-1)(r-1)}$$

$$M_{\rm GW}^2 > 0 \,.$$

$$\begin{aligned}
&[0 < X < 1 \quad \text{and} \quad 1 < r \le \bar{r} \quad \text{and} \quad 0 < \omega < 6] \\
\text{or} \quad &[0 < X < 1 \quad \text{and} \quad r > \bar{r} \quad \text{and} \quad 0 < \omega < \bar{\omega}] \\
\text{or} \quad &[X > 1 \quad \text{and} \quad \bar{\omega} < \omega < 6] \,,
\end{aligned}$$

Extended Quasidilaton

$$3H^2 - \frac{\omega}{2}\dot{\sigma}^2 = \Lambda + \Lambda_X + \frac{1}{M_{\rm Pl}^2}\rho_M\,, \quad (5)$$

$$\dot{H} = \frac{1}{6}(q-1)\frac{\dot{\Lambda}_X}{\dot{\sigma}-H} - \frac{\omega}{2}\dot{\sigma}^2 - \frac{1}{2M_{\rm Pl}^2}(\rho_M + P_M)\,. \quad (6)$$

$$w_x = -1 + \frac{w\dot{\sigma}^2 - m_g^2(r-1)X[J + X(\alpha_3(X-1)-2)]}{\frac{\omega}{2}\dot{\sigma}^2 + m_g^2(X-1)[J + (X-1)(\alpha_3(X-1)-3)]}$$

Supernovae Data

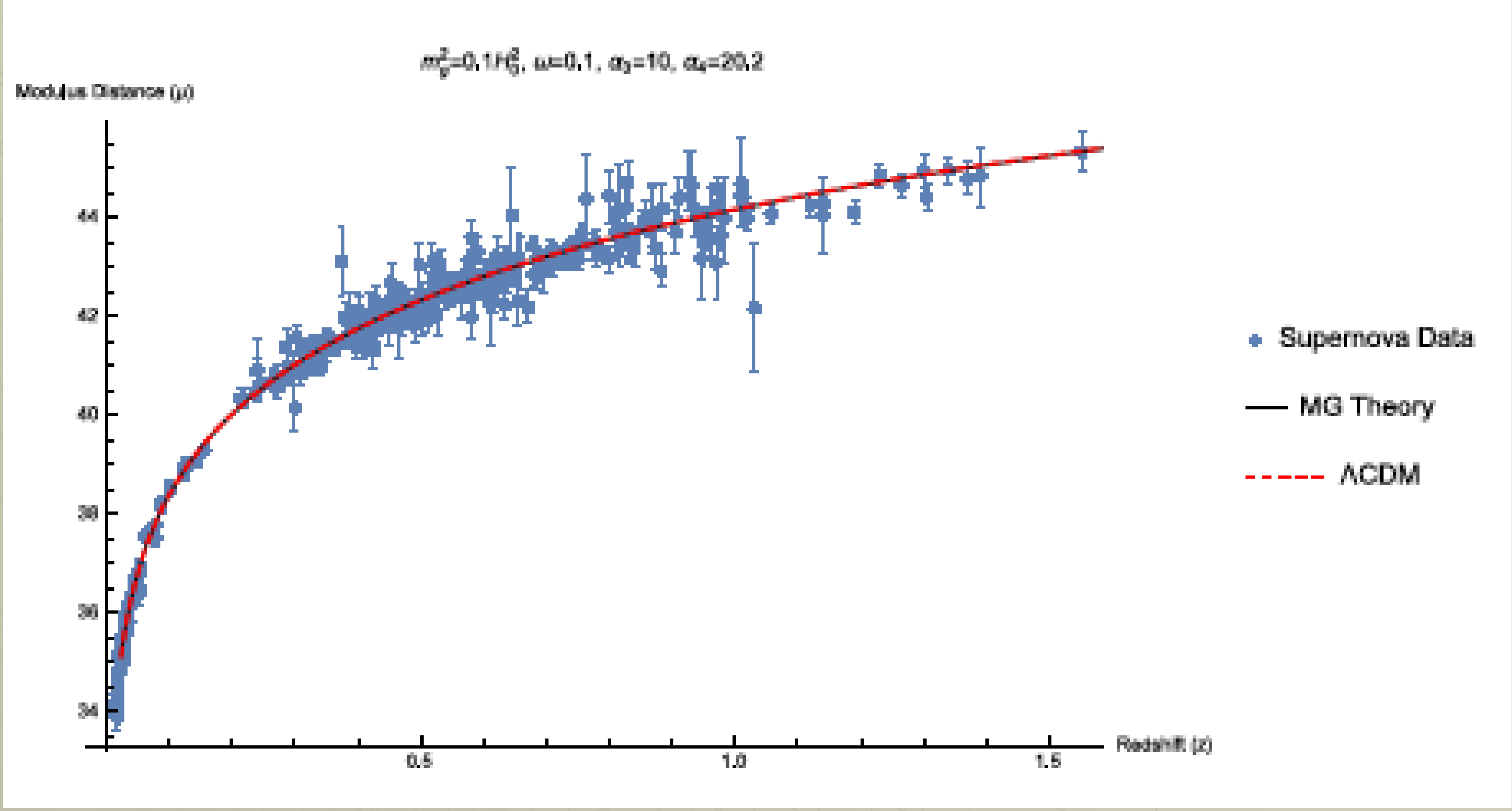

Extended Quasidilaton Massive Gravity

$$\left(\frac{\dot{\phi}^0}{n}\right)^2 \equiv 1 - \alpha_\sigma \left(\frac{\dot{\sigma}}{qXm_g}\right)^2 ,$$

$$\frac{\partial}{\partial t}\left[\frac{a^4\dot{\phi}^0}{n} JX(1-X)\right] = 0.$$

$$\partial_t\left[(1 - \frac{\alpha_\sigma (H+Y)^2}{m_g^2 X^2 r^2})^{\frac{1}{2}} a^4 JX(X-1)\right] = 0$$

Constraint Equation

$$\frac{m_g^2 X r}{H+Y}\left[4JH(X-1)+Y\left[3X(\alpha_3(X-1)-2)+J(4X-1)\right]\right] = \frac{\alpha_\sigma}{Xa^4}\frac{d}{dt}\left\{\frac{a^4}{r}(H+Y)J(X-1)\right)\right\} \quad (5)$$

$$\frac{\dot{X}}{X} = \frac{4(1-X)JH}{3X(\alpha_3(X-1)-2)+J(4X-1)}\,, \qquad (7)$$

J=0

$$(3-\frac{\omega}{2})H_J^2=\Lambda_J+\frac{1}{M_{\rm Pl}^2}\rho_M\ ,$$

$$\dot{H}_J=\frac{1}{2}m_g^2(r_J-1)X_J^2(\alpha_3(X_J-1)-2)]-\frac{\omega}{2}H_J^2+\frac{1}{2M_{\rm Pl}^2}(\rho_M+P_M).$$

$$r_J=1+\frac{\omega(\dot{H}_J+3H_J^2)}{3m_g^2X_J^2[\alpha_3(X_J-1)-2]}$$

$$\alpha_\sigma>\frac{r_A^2\left[(3-\frac{\omega}{2})X_A^2[\alpha_3(X_A-1)-2]+\omega(X_A-1)^2[\alpha_3(X_A-1)-3]\right]^2}{X_A^2(X_A-1)^2[\alpha_3(X_A-1)-2]^2(3-\frac{\omega}{2})[\alpha_3(X_A-1)-3]}$$

Note that the upper bound of α_σ is determined through the background stability $((\dot{\phi}^0/n)^2>0$ and it is given by

$$\alpha_\sigma<\frac{m_g^2X^2r^2}{\dot{\sigma}^2} \tag{37}$$

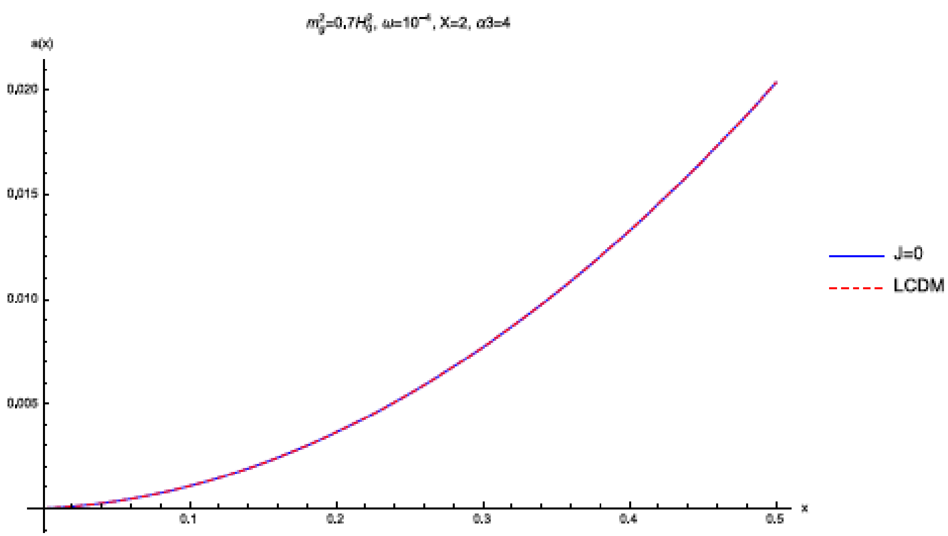

m_g^2=0,7H_0^2, ω=10^{-4}, X=2, α3=4
a(x)
0,020
0,015
0,010
0,005
0.1
0.2
0.3
0.4
0.5
x
J=0
LCDM

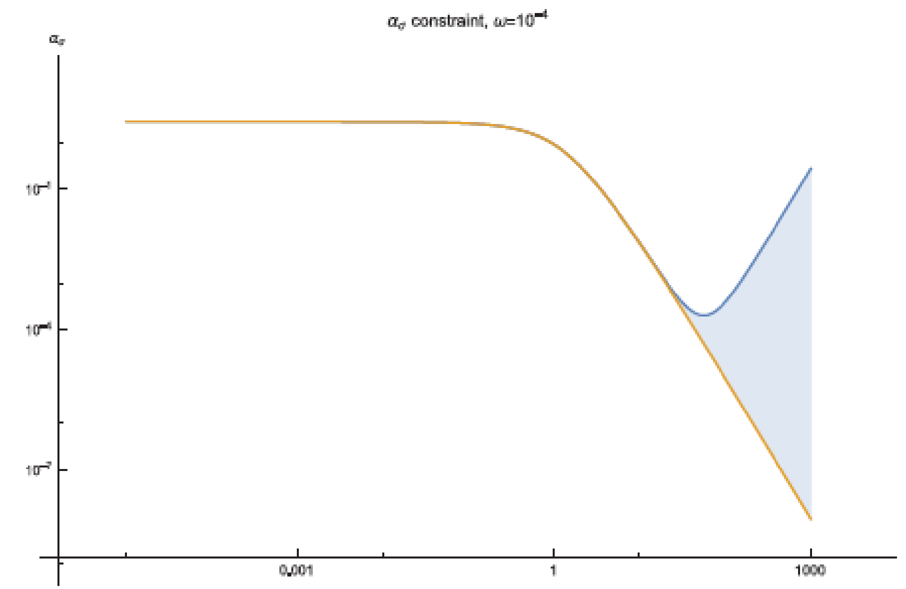

α_σ constraint, ω=10^{-4}
α_σ
10^{-1}
10^{-4}
10^{-7}
0,001
1
1000
z

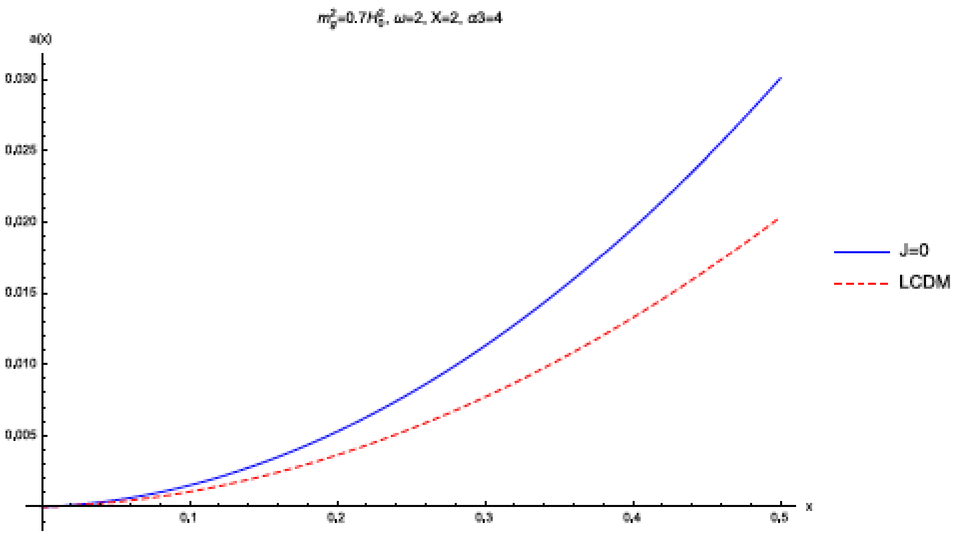
m_g^2=0.7H_0^2, ω=2, X=2, α3=4
a(x)
0,030
0,025
0,020
0,015
0,010
0,005
0,1
0,2
0,3
0,4
0,5
x
J=0
LCDM

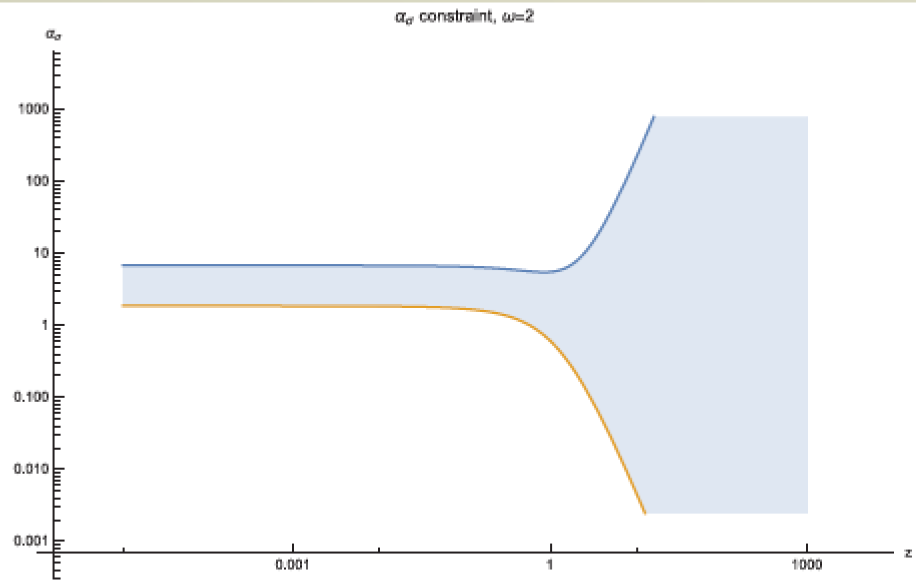
α_σ constraint, ω=2
α_σ
1000
100
10
1
0.100
0.010
0.001
0.001
1
1000
z

J non-zero

- Initial conditions
  - We do not know how the quasidilaton field behaves
- *Anselmi et al. 2017*: Faillures of homogeneous solutions

Failures of homogeneous and isotropic cosmologies in Extended Quasi-Dilaton Massive Gravity

Stefano Anselmi,[1,2,3,*] Saurabh Kumar,[3,†] Diana López Nacir,[4,‡] and Glenn D. Starkman[3,§]

[1]*LUTH, UMR 8102 CNRS, Observatoire de Paris, PSL Research University, Université Paris Diderot, 92190 Meudon – France*

[2]*Institut d'Astrophysique de Paris, CNRS UMR 7095 and UPMC, 98bis, bd Arago, F-75014 Paris – France*

[3]*Department of Physics/CERCA/Institute for the Science of Origins, Case Western Reserve University, Cleveland, OH 44106-7079 – USA*

[4]*Theoretical Physics Department, CERN, CH-1211 Genève 23, Switzerland*

(Dated: June 7, 2017)

We analyze the Extended Quasi-Dilaton Massive Gravity model around a Friedmann-Lemaître-Robertson-Walker cosmological background. We present a careful stability analysis of asymptotic fixed points. We find that the traditional fixed point cannot be approached dynamically, except from a perfectly fine-tuned initial condition involving both the quasi-dilaton and the Hubble parameter. A less-well examined fixed-point solution, where the time derivative of the 0-th Stückelberg field vanishes $\dot{\phi}^0 = 0$, encounters no such difficulty, and the fixed point is an attractor in some finite region of initial conditions. We examine the question of the presence of a Boulware-Deser ghost in the theory. We show that the additional constraint which generically allows for the elimination of the Boulware-Deser mode is *only* present under special initial conditions. We find that the only possibility corresponds to the traditional fixed point and the initial conditions are the same fine-tuned conditions that allow the fixed point to be approached dynamically.

Cosmological Signatures: CMB

- Temperature anisotropies

$$S_\theta = -\dot{h}e^{-\tau} + g\Phi$$

- Massive gravity - ISW

- Polarization

$$S_P = g\Phi$$

Imprints on CMB?

- At high densities GR is recovered and perturbations look like as LCDM
- Late time evolution –ISW
- Suppression

exp(-mR)?

- Anisotropic Bianchi model(s) ONLY at large scales

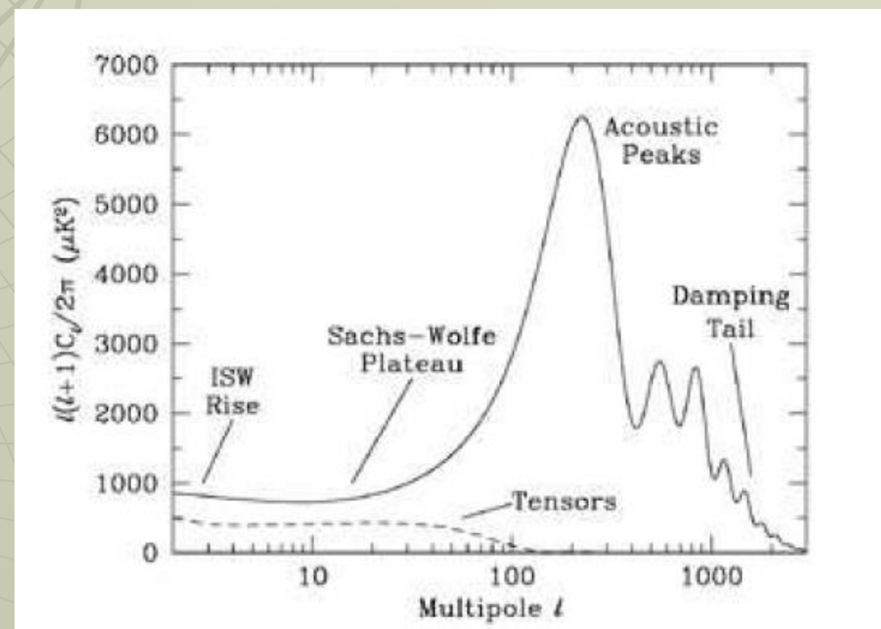

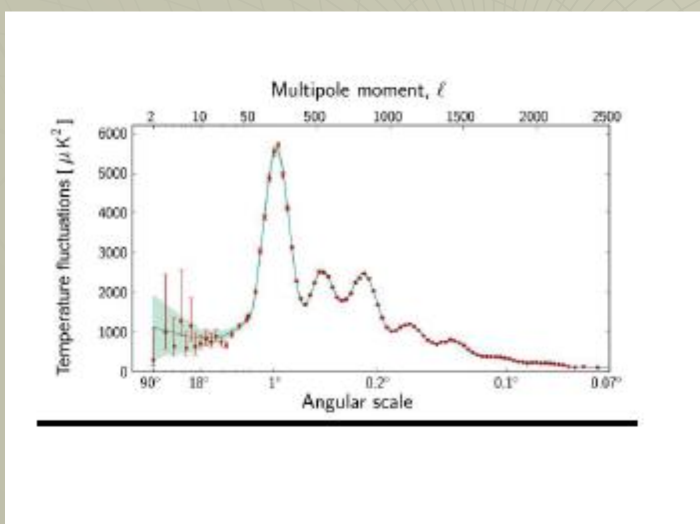

$$\frac{\Delta T}{T}(\vec{n}) \approx \phi_e(\vec{n}) + \int_e^o \frac{\partial \phi}{\partial t} dt + \vec{n}\cdot(\vec{v}_o - \vec{v}_e) + \left(\frac{\Delta T}{T}(\vec{n})\right)_e$$

Gravitational Waves

- Analytical approach:

Review by *Pritchard and Kamionkoswki* 2004

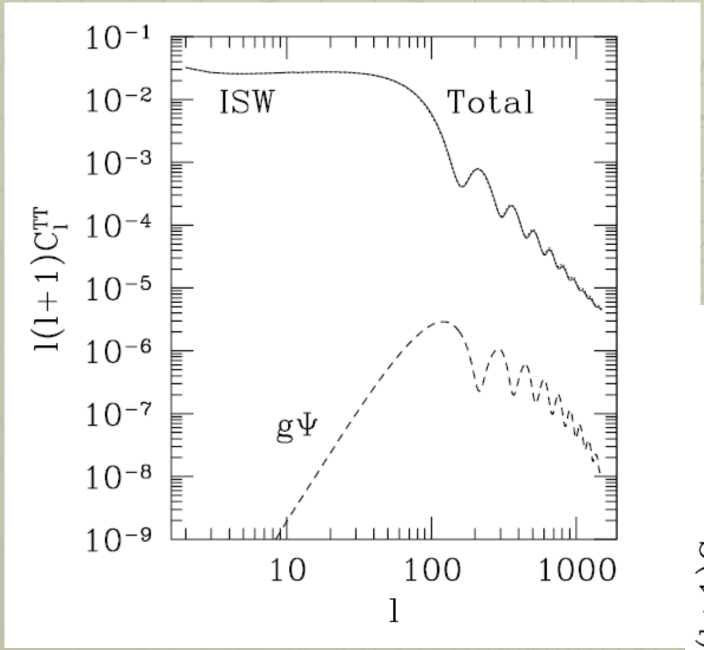

$$P_h(k) = A_T k^{n_T - 3},$$

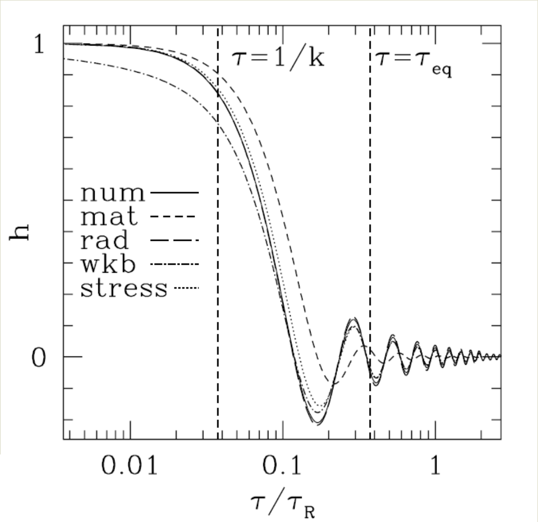

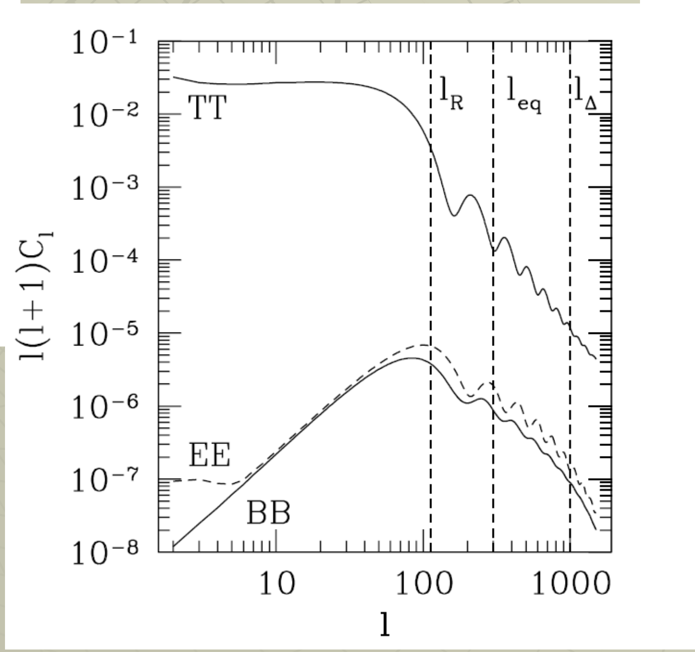

$$h \propto \begin{cases} 1, & k < 1/\tau_0, \\ k^{-2}, & 1/\tau_{\rm eq} > k > 1/\tau_0, \\ k^{-1}, & k > 1/\tau_{\rm eq}. \end{cases}$$

$$l(l+1)C_l^{TT} \propto \begin{cases} 1, & l < l_R, \\ l^{-4}, & l_{\rm eq} > l > l_R, \\ l^{-2}, & k > l_{\rm eq}. \end{cases}$$

Gravitational Waves

$$\omega^2 = \frac{k^2}{a^2} + M_{GW}^2 \,,$$

Gumrukcuoglu et al. 2012

$$\bar{\gamma}_k'' + \left(c_g^2 k^2 + a^2 M_{GW}^2 - \frac{a''}{a} + 2K c_g^2 \right) \bar{\gamma}_k = 0, \quad \bar{\gamma}_k \equiv a \gamma_k,$$

$$\frac{\mathcal{P}(\omega_0)}{\mathcal{P}_{GR}(\omega_0)} = \frac{\mathcal{P}_{prim}(k)}{\mathcal{P}_{prim}(k')} \mathcal{S}^2(\omega_0),$$

$$\mathcal{S}(\omega_0) = \frac{k' a_k}{k\, a_{k'}^{GR}} \sqrt{\frac{\omega_k a_k}{\omega_0 a_0}}, \quad k = a_0 \sqrt{\omega_0^2 - M_{GW,0}^2}, \quad k' = a_0 \omega_0.$$

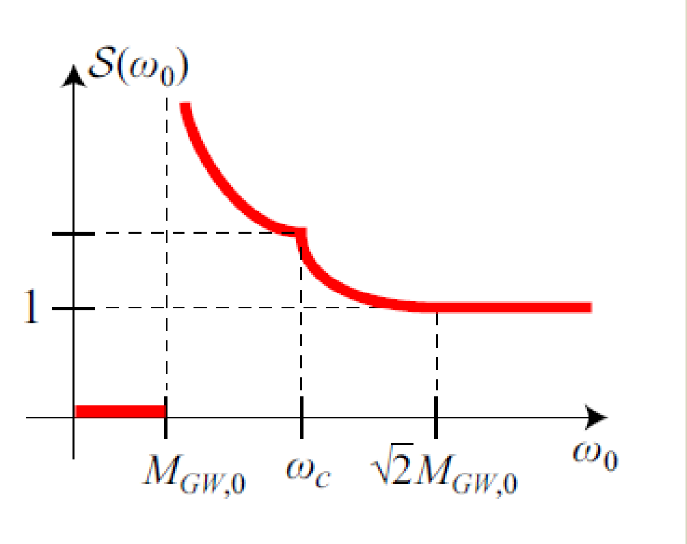

- No modification in the high frequency range ($k_0 < k \Leftrightarrow \sqrt{2}M_{GW,0} < \omega_0$): $\mathcal{S}(\omega_0)$ stays almost unity.
- Modest enhancement in the intermediate frequency range ($k_c < k < k_0 \Leftrightarrow \omega_c < \omega_0 < \sqrt{2}M_{GW,0}$): $\mathcal{S}(\omega_0)$ is proportional to some positive powers of $(\omega_0^2 - M_{GW,0}^2)^{-1}$ as shown in Eq. (55), and thus increases as ω_0 decreases.
- Sharp peak just above the cutoff ($0 < k < k_c \Leftrightarrow M_{GW,0} < \omega_0 < \omega_c$): $\mathcal{S}(\omega_0)$ is proportional to $(\omega_0^2 - M_{GW,0}^2)^{-1/2}$, and thus it diverges in the limit $\omega_0 \to M_{GW,0}$.
- No signal below the cutoff ($\omega_0 < M_{GW,0}$): $\mathcal{S}(\omega_0) = 0$.

Massive Gravity: CMB

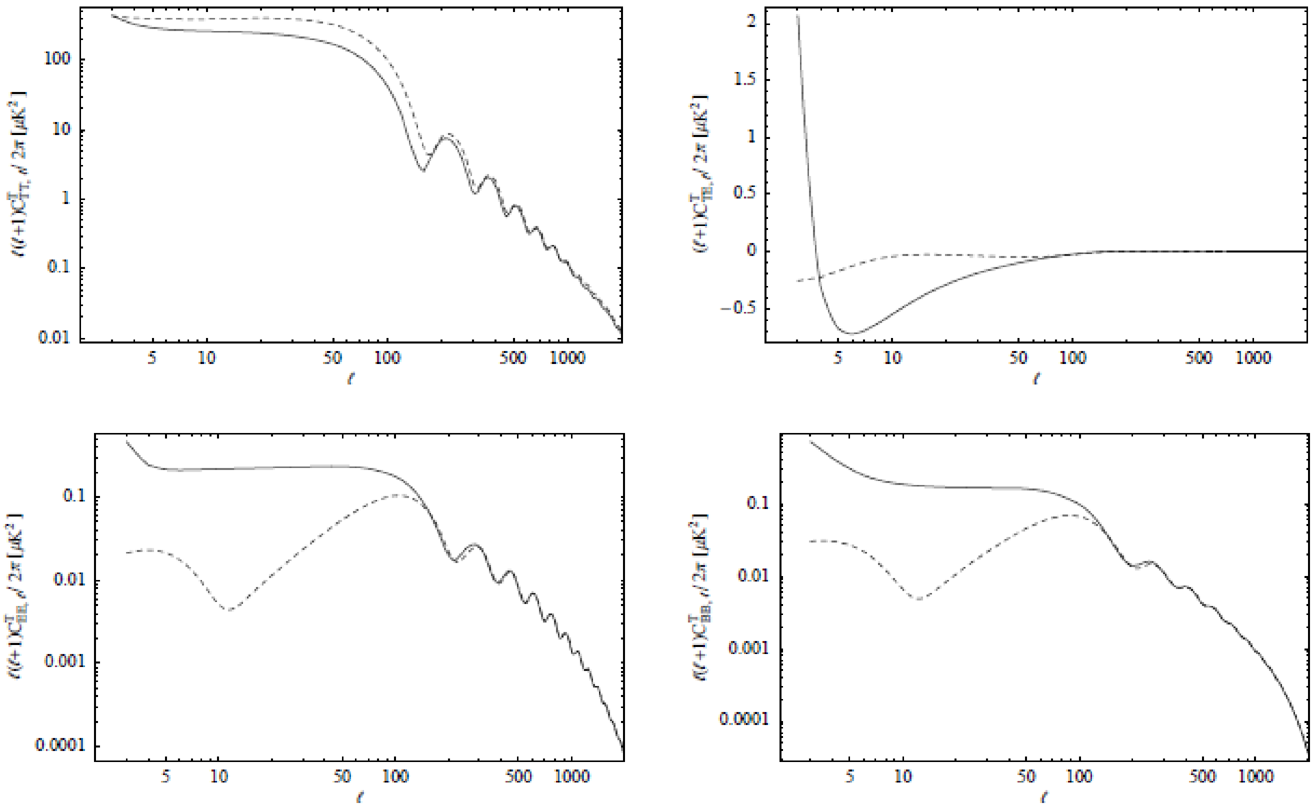

Dubovsky et al. 2009

Figure 4: This plot shows T (upper left panel), E (lower left), TE (upper right) and B (lower right) spectra for the massive case with $\mu = 10$ (solid line) and for the massless case (dashed line).

Quasidilaton Massive Gravity

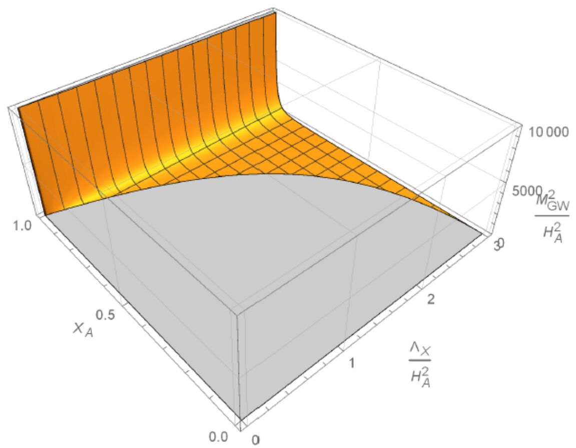

FIG. 1: (Color online) Plot of M^2_{GW}/H^2_A in the entire region for $0 < X_A < 1$.

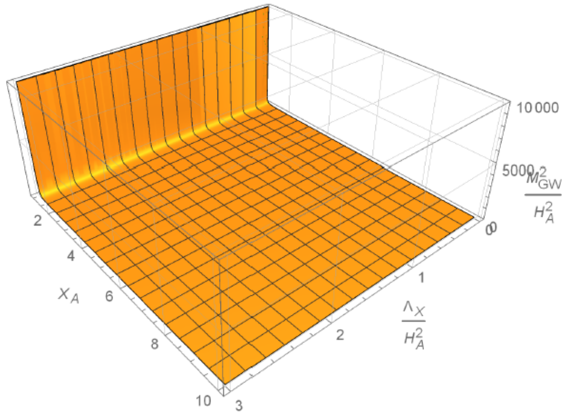

FIG. 2: (Color online) Same as Fig. 1, but for $X_A > 1$.

$$M^2_{GW} \equiv \frac{(q-1)X^3 m_g^2}{X-1} + \frac{\omega H^2[(q-1)(X+1)+X-1]}{(X-1)(q-1)}$$

$$\bar{q}_A = \frac{2}{X_A+1} - \frac{\omega}{X_A(1+X_A)}\left[\frac{\frac{m_g}{H_A}(X_A-1)^2}{(3-\frac{\omega}{2})+\frac{m_g^2}{H_A^2}(X_A-1)^2}\right]^2 \quad (12)$$

$$0 < X_A < 1\,, \quad 1 < q_A < \bar{q}\,, \quad 0 < \omega < 6$$

Kahniashvili, et al. 2015

Cosmological Tests: Lensing

- *Spolyar et al. 2013*

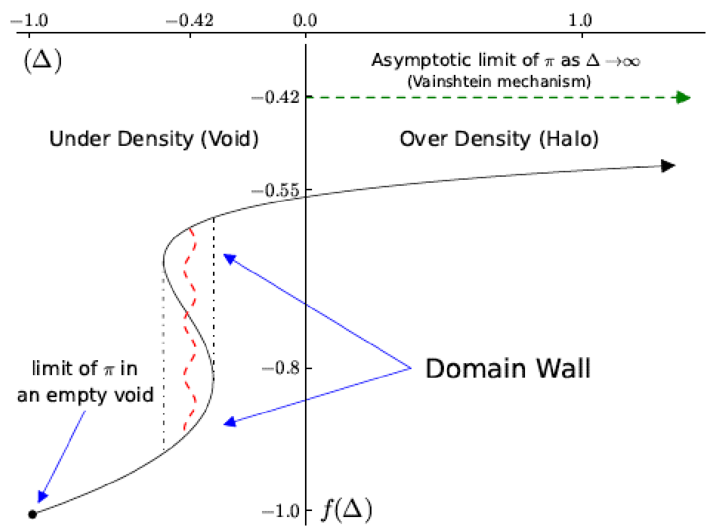

FIG. 1: Plot of f with $\pi'/r = f(\Delta)\Lambda^3$ where $\Delta = \delta\rho_m/\rho_{m0}$ is the difference between the mean density inside of a radius r and the mean density today normalized by the mean density today. The vertical black dashed lines indicate the domain wall region. The wiggly red dashed line is meant to indicate that a field transition between branches takes place within the region.

- Gravitational lensing enhancement in screened and un-screened regions

Cosmological Signatures

- Wyman et al. 2011, 2013

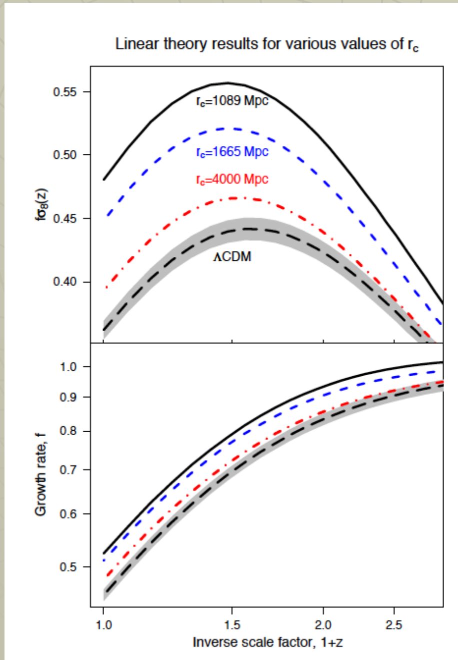

FIG. 5. The linear growth rate – both weighted by $\sigma_8($ and alone – as a function of redshift, z, for ΛCDM, th r_c = 1089 Mpc and r_c = 1665 Mpc galileon models, pl a comparison model with r_c = 4000 Mpc, are shown as black dashed line, a solid black line, a dashed blue line, an a dash-dotted red line, respectively. The grey band arour the ΛCDM line represents the expected precision of futu surveys, which hope to achieve ±2% accuracy in their me surement of the growth rate.

- Gravitational clustering (due to additional fifth force)
  - Growth rate
  - Halos abundance

$$\Psi_{\rm dyn} = \Phi_N + \frac{1}{2}\varphi.$$

Graviton Mass Limits

- Pulsar timing

  $m_g < 10^{-20}$eV

  Taylor 1994

- Gravitational waves

  10^{-22} -10^{-23}eV

  De Rham 2015

- Solar system:

  $m_g < 10^{-22}$eV

  Keppel & Ajit 2010

  Gruzinov 2001

- Cosmology effects

  10^{-30} -10^{-33}eV

  De Rham 2015

Conclusions

- Are large scale anomalies physical?
  - Cosmological origin?
- If yes do we see new physics at large scales?
  - Early Universe
  - Late time
- Massive gravity manifestation?
  - CMB fluctuations formation
  - CMB Polarization

Thank you!
Spacial Thanks to:

- Organizers, in particular:
  - Akaki Ruzetski
  - Mirian Tabidze
- Collaborators:
  - Nishant Agarwal
  - Arjun Kar
  - Arthur Kosowsky
  - George Lavrelashvili
  - Paul Rogozenski
- And for discussions:
  - Tiziana Di Matteo
  - Giga Gabadadze
  - Justin Khoury
  - Danielle Leonard
  - Dato Pirtskhalava